Axial oxygen vacancy-regulated microwave absorption in micron-sized tetragonal BaTiO₃ particles

Kyungnae Baek, [a] Seungyong Lee,[b] Sang-Gil Doh,[c] Miyoung Kim,[b] Jerome K. Hyun*[a]

[a] Department of Chemistry and Nanosicence, Ewha Womans University, Seoul, Korea

[b] Department of Materials Science and Engineering and Research Institute of Advanced Materials, Seoul National University, Seoul, Korea

[c] R&D Center, YoulChon Chemical, Co., Ltd., 112, Yeouidaebang-ro 24-gil, Dongjak-gu, Seoul, Korea

*E-mail: kadam.hyun@ewha.ac.kr.
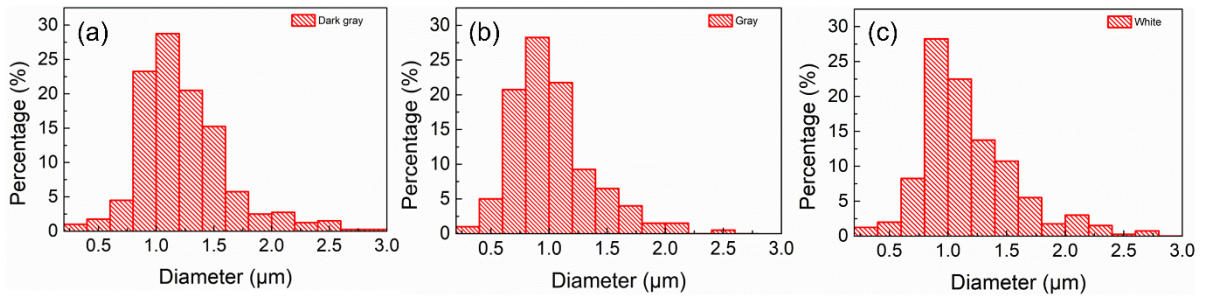
Table of Contents

Fig. S1. Size distribution of BTO sets. Measured size distribution of the (a) dark gray, (b) gray, and (c) white BTO particles. The mean particle sizes of the three samples are similar.

Physical and chemical properties of BTO particles sets

To elucidate the crystalline nature of the particles, bright-field TEM images of the three particle sets and selected area electron diffraction patterns from representative areas were obtained, as shown in Fig. S2a-c and their insets, respectively. The particles were embedded in an epoxy matrix and milled by a focused ion beam to an electron-transparent thickness. In all cases, the bulk region of the particles was found to be highly crystalline, regardless of the degree of reduction, as can be seen from the diffraction patterns.

XRD measurements were performed on the three sets, as shown in Fig. S2d, to obtain the crystallographic phase of the bulk powder and to evaluate grain size of the particles. In Fig. S2d, a tetragonal crystal phase was observed in all sets. Debye-Scherrer analysis of the strongest (110) diffraction peaks shown in Table S1 reveals similar average particle sizes of 45.4, 52.1 and 50.7 nm, respectively, for dark gray, gray and white particles.

The discoloration of titanates due to the incorporation of oxygen vacancies from reduction is a well-established phenomenon,[1,2] and can be used as a gauge for roughly assessing their relative concentration. Oxygen vacancies are known to produce midgap electronic states, which account for the dark appearance of oxygen-deficient titanates in the visible range.[3] To assess the discoloration, we evaluated the diffuse reflectance spectra (DRS) from the three particle sets, as shown in Fig. S2e. Bandgap energies derived from Kubelka-Munk analysis on each spectrum were found to be consistent, with a value of 3.12±0.02eV. Up to the bandgap onset of ~397 nm , all three particle sets consistently reflected less than 20% of light due to the strong interband absorption. Above 397 nm and into the near IR, clear differences in diffuse reflectance among the particle sets were displayed as can be seen from the 45, 75 and 100% reflection for the dark gray, gray and white particles, respectively. Such a trend signifies increased visible light absorption and hence increased darkness in the appearance of the more

reduced particles.

To determine the presence of Na, K, Cl ions and other impurities in the BTO particles, STEM / EDX measurements were performed on the two extrema samples (white, dark gray particles) and bare epoxy resin. Figure S3 shows data from representative particles from each particle set. As can be seen from the epoxy analysis, the small trace of Cl and signal from C can be attributed to the epoxy background. Si is detected as a component of the EDS detector. Cu is detected from the TEM grid. And the Ga signal is due to the Ga ion used during FIB sampling. A small trace of Na was detected in the particles due to the use of salt precursors during synthesis. The concentration ratio of Na atoms relative to Ba atoms, obtained from measurements from multiple particles and regions was 0.012 ± 0.002 for the dark gray particles and 0.011 ± 0.003 for the white particles.
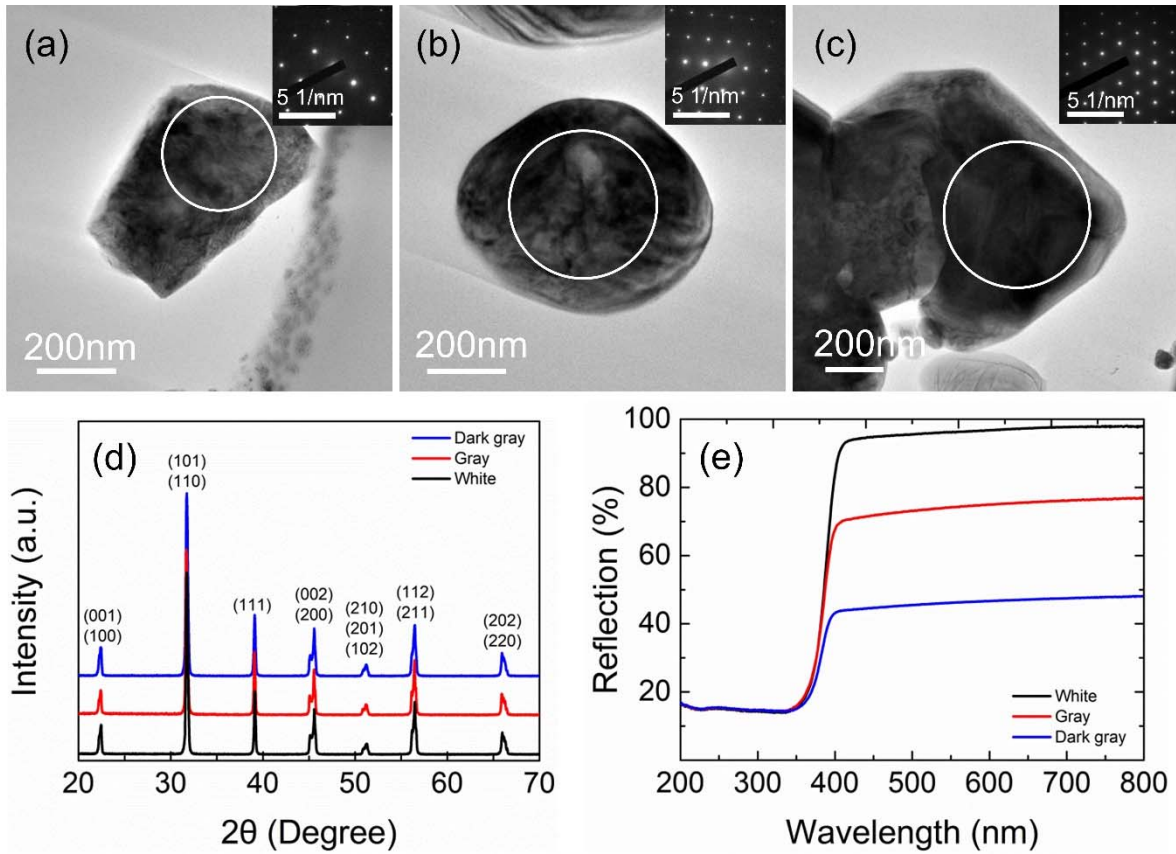
Fig. S2. Bright-field TEM images of representative (a) dark gray, (b) gray, and (c) white BTO particles. Scale bar is 200nm. Inset: SAED patterns from the white circled areas. Inset scale bar is 5 nm^{-1}. (d) X-ray diffraction spectra and (e) diffuse reflectance spectra of the dark gray, gray, and white BTO particles

Sample name	2-Theta	FWHM	Grain size (nm)	Particle size (μm)
Dark gray	31.72 (0.003)	0.208 (0.004)	45.4	1.19
Gray	31.69 (0.003)	0.187 (0.005)	52.1	1.04
White	31.73 (0.003)	0.191 (0.004)	50.7	1.18

Scherrer's equation

$$B(2\theta) = \frac{K\lambda}{\beta\cos\theta}$$

$\lambda \rightarrow$ Wavelength of X-ray

$\beta \rightarrow$ Full width at half maxima

Table S1. Calculated grain size of BTO particle sets from Debye-Scherrer's equation and the measured XRD data
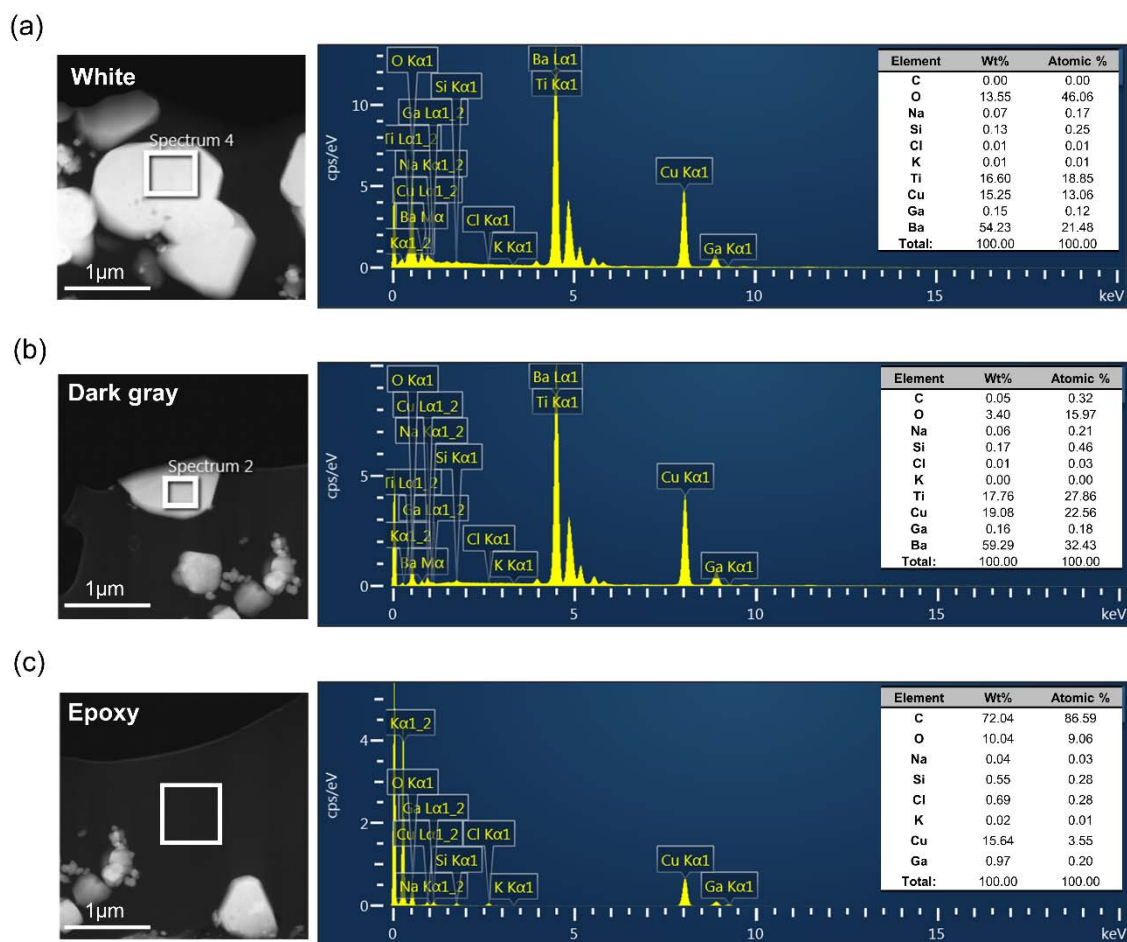
(a)

(b)

(c)

Fig. S3. STEM image (left) and EDX spectrum (right) of (a) white, (b) dark gray particles and (c) bare epoxy.

Permittivity and permeability of BTO particle sets

To investigate the effect of oxygen vacancies on the microwave absorption properties of BTO particles, each BTO particle set was dispersed in a polyurethane (PU) with a load of 60% by weight and the complex permittivity and permeability of the composite material were evaluated in the GHz range. We prepared several specimens of slightly different thicknesses in each set of particles to ensure the accuracy of the measurements. Ideally, the same composites with different thicknesses should produce the same complex permittivity and permeability. Fig. S4 shows the permittivity of the dark gray, gray and white particle composites of different thicknesses. Fig. S5 present the complex permeability of the dark gray, gray and white BTO particle composites. Each curve represents the averaged magnetic function from identical composites of different thicknesses. Fig. S6 shows the complex permittivity and permeability of PU with a 2.4mm thickness from 1 to 18 GHz.
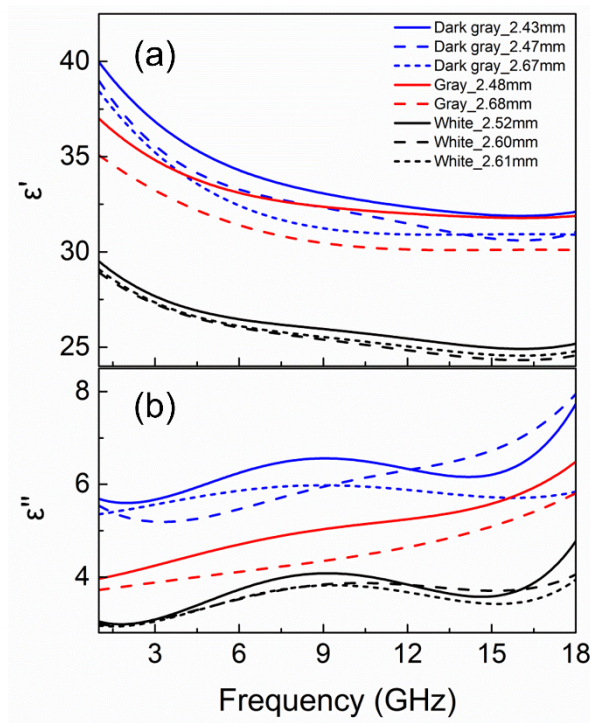
Fig. S4. Frequency dependence of (a) the real and (b) imaginary part of the complex permittivity of BTO particles/ PU composites with different thicknesses.
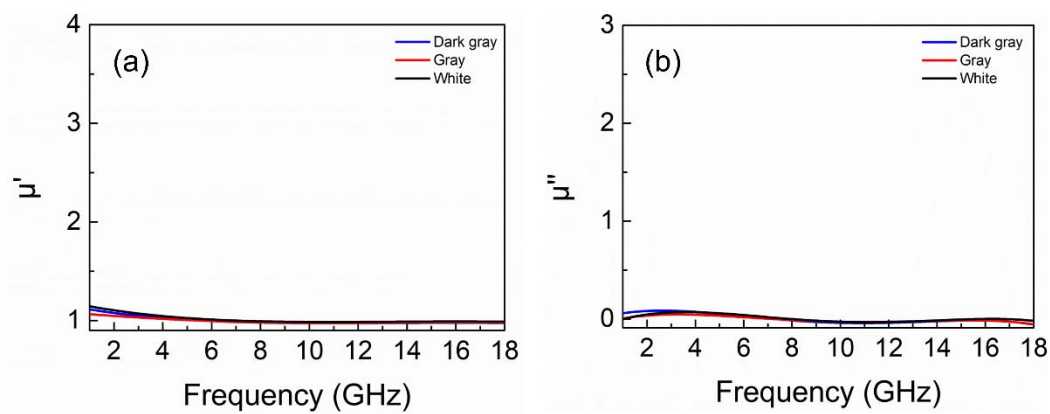

Fig. S5. Frequency dependence from 1 to 18 GHz of (a) the real and (b) imaginary part of complex permeability of dark gray, gray and white BTO particles/ PU composites
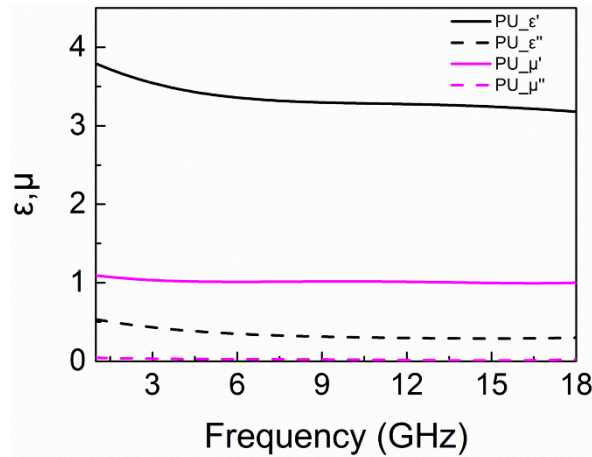
Fig. S6. Frequency dependence from 1 to 18 GHz of the complex permittivity and permeability of PU with a 2.4mm thickness.

Reflection loss of BTO particle sets

Reflection loss spectra of the three types of composites using a type N 50 ohm airline equipped with a reflecting backplate and were also obtained experimentally from a 1-port setup. Use of this type of coaxial transmission line has become standard practice in industry due to its utility in providing EMI shielding efficiency, S parameters, complex permittivity and permeability values using the same configuration. The main difference to traditional coaxial transmission line for reflection loss measurements is the presence of an air buffer layer between the reflecting backplate and the sample. Fig.S7 provides the measured results for the three types of composites with slightly different thicknesses close to 2.5 mm. One can find that this method results in changes in the reflection loss peak positions compared to those from the traditional method due to multiple reflections introduced by the extra air layer. Comparison among the three types of composites shows that darker particles can enhance microwave absorption at 10 GHz from -15dB for the white particle composites to -25dB for the dark gray particle composites.

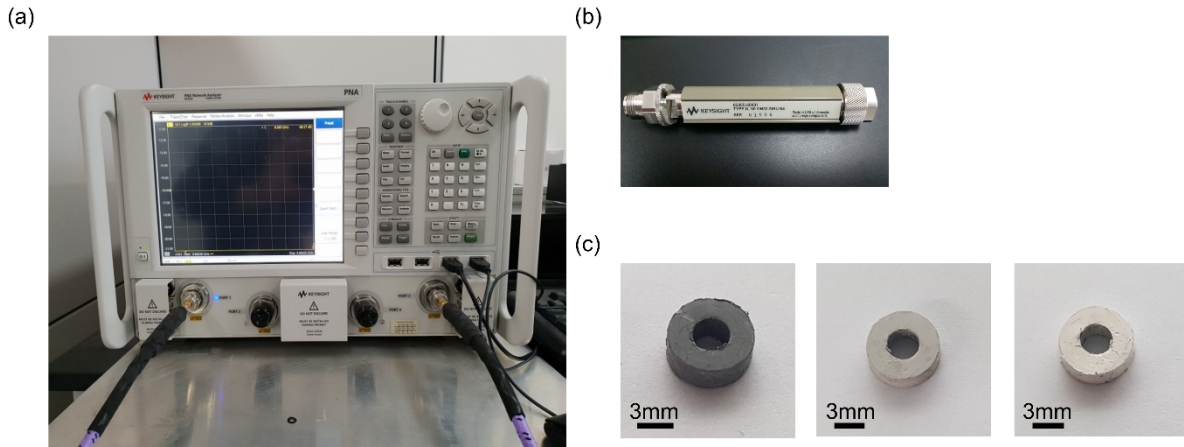**Microwave absorption property measurement**

Fig. S7. (a) PNA network analyzer (N5225A) and (b) Type N 50 ohm airline fixture (85055-60001) for measurement of complex permittivity, permeability and reflection loss of BTO particles/PU composites. (c) BTO particles/PU composites molded into toroidal-shaped samples for measurement with the coaxial transmission line. Scale bar is 3mm. The internal and external diameters of the composite are 3mm and 7mm, respectively.
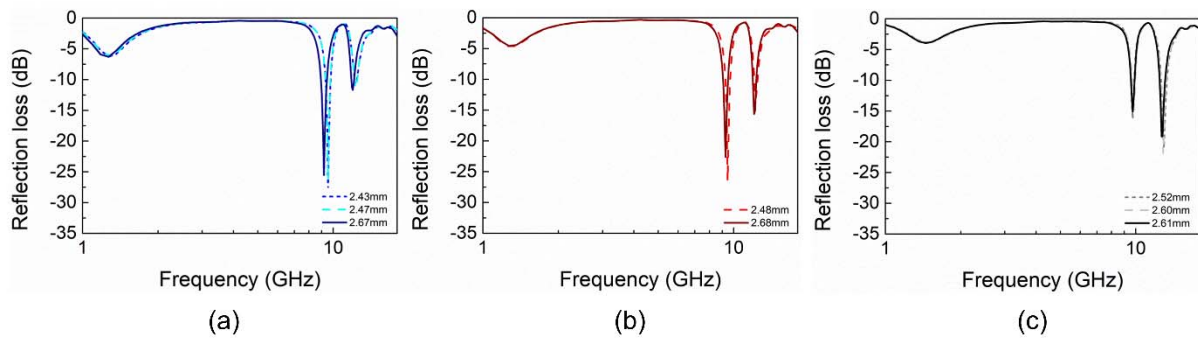

Fig. S8. The measured reflection loss spectra of (a) dark gray, (b) gray, and (c) white BTO particles/PU composites in the microwave region using a type N 50 Ohm airline fixture capped by a reflecting backplate. There exists an air layer between the composite and reflecting backplate. Each spectrum represents a composite of different thickness.

References

1. H. Cui, W. Zhao, C. Yang, H. Yin, T. Lin, Y. Shan, Y. Xie, H. Gu and F. Huang, *J. Mater. Chem. A*, 2014, **2**, 8612-8616.
2. R. C. Pullar, S. J. Penn, X. Wang, I. M. Reaney and N. M. Alford, *J. Eur. Ceram. Soc*, 2009, **29**, 419-424.
3. X. Chen, L. Liu, P. Y. Yu and S. S. Mao, *Science*, 2011, **331**, 746-750.